Journal of Zhejiang University SCIENCE A
ISSN 1673-565X (Print); ISSN 1862-1775 (Online)
www.zju.edu.cn/jzus; www.springerlink.com
E-mail: jzus@zju.edu.cn

Bifurcation and chaos of a 4-side fixed rectangular thin plate in electromagnetic and mechanical fields*

Wei-guo ZHU†[1,2], Xiang-zhong BAI[1]

([1]*School of Civil Engineering and Mechanics, Yanshan University, Qinhuangdao 066004, China*)

([2]*Department of Transportation Engineering, Huaiyin Institute of Technology, Huai'an 223001, China*)

†E-mail: bobweiguo@sina.com

Received Feb. 23, 2008; Revision accepted July 2, 2008; Crosschecked Oct. 29, 2008

Abstract: We studied the problem of bifurcation and chaos in a 4-side fixed rectangular thin plate in electromagnetic and mechanical fields. Based on the basic nonlinear electro-magneto-elastic motion equations for a rectangular thin plate and the expressions of electromagnetic forces, the vibration equations are derived for the mechanical loading in a steady transverse magnetic field. Using the Melnikov function method, the criteria are obtained for chaos motion to exist as demonstrated by the Smale horseshoe mapping. The vibration equations are solved numerically by a fourth-order Runge-Kutta method. Its bifurcation diagram, Lyapunov exponent diagram, displacement wave diagram, phase diagram and Poincare section diagram are obtained.

Key words: Rectangular thin plate, Electromagnetic-mechanical coupling, Melnikov function method, Runge-Kutta method, Bifurcation, Chaos

doi:10.1631/jzus.A0820132 **Document code:** A **CLC number:** O34

INTRODUCTION

The rectangular thin plates are widely used in engineering structures, such as machinery, shipbuilding, aeronautic-astronautic, watercraft-hydropower, and civil engineering. Usually, these thin plates work under the conditions of mechanical fields, electromagnetic fields and thermal-elastic fields (Bai, 1996a). Therefore, a full understanding of their dynamics is crucial to developing high-tech constructions and mechanisms, and a well study on the vibration of thin plates coupled with various fields is very important.

Many scholars have done numerous studies of the thermal-elastic coupling theory (Nowacki, 1975; Chang and Wang, 1986; Trajkorski *et al.*, 1999). The exact solution for the simply supported multilayered and functionally graded magneto-electro-elastic plates was made by Pan (2001), Pan and Heyliger (2002), Pan and Han (2005), and Wang *et al.*(2003).

In recent years, chaos theory has been a newly developed research subject (Chen, 1993; Huang, 2000). Although chaotic vibrations exhibited by plates have been less analyzed, recently they have been studied more intensively. Many scholars have researched intense chaotic motion in all kinds of components subjected to mechanical forces, and have made great progress. Zhang *et al.*(2001) used the Galerkin method to derive averaged equations from the von Karman equation, and analyzed both local and global bifurcations of a parametrically and externally excited simply supported rectangular thin plate. Awrejcewicz *et al.*(2003) analyzed bifurcation and routes to chaos exhibited by thin plate strips. Jump-like switching phenomena, series of bifurcations, a route to chaos and various types of strange chaotic attractors have been reported and discussed. Awrejcewicz *et al.*(2004) reported the mechanism of transition to chaos of deterministic systems with an infinite number of degrees of freedom using the examples of paths for parametric vibrations of flexible rectangular plates. Regular and chaotic vibrations and

* Project (No. A2006000190) supported by the Natural Science Foundation of Hebei Province, China

bifurcations of flexible plate strips with non-symmetric boundary conditions were investigated through the Bubnov-Galerkin and finite difference method by Awrejcewicz *et al.*(2006). Some new examples of the paths from regular to chaotic dynamics within chaotic dynamics were illustrated and discussed by them. The phase transitions from chaos to hyper chaos, and a novel phenomenon of a shift from hyper chaos to hyperhyper chaos were reported also. To the authors' understanding, the study of bifurcation and chaos coupled with mechanical fields and magneto-electro fields was rarely reported.

In our investigation of the nonlinear dynamics of rectangular thin plates, we obtained a decoupled modal form of equation of motion by the Galerkin's method for certain geometries and boundary conditions. By this approach, we establish the modal Duffing equation for a rectangular thin plate subject to steady electromagnetic and mechanical loading in the 4-side clamped boundary condition. In this paper, the problem of bifurcation and chaos of a 4-side fixed rectangular thin plate in electro-magnetic and mechanical fields is studied. Based on basic nonlinear electro-magneto-elastic motion equations for rectangular thin plates and expressions of electromagnetic forces, the vibration equations of the rectangular thin plate under the action of a mechanical field and a steady transverse magnetic field are derived. By using the Melnikov function method, the chaos condition and limitation of the system under the condition of Smale horseshoe map are given. Using the fourth-order Runge-Kutta method the vibration equations will be solved numerically. For some examples, the bifurcation diagram, the Lyapunov exponent diagram, the displacement wave diagram, the phase diagram and the Poincare section diagram of the system will be obtained. The influences of the electromagnetic field and mechanical loads on the system vibration will be analyzed. We illustrate thin plate behaviors by numerical results in electromagnetic and mechanical vibrations.

EQUATIONS OF MOTION

Consider a rectangular thin plate in a steady electromagnetic field $\bar{\boldsymbol{B}}(B_x, B_y, B_z)$ and loaded by a uniformly distributed mechanical force $\bar{\boldsymbol{P}}(P_1, P_2, P_3)$. In the right-angle Cartesian coordinate system (*OXYZ*), *OXY* is the neutral plane, *Z* is its normal. By ignoring influences such as thermal effects, polarization and magnetization, and assuming that the electromagnetic field intensities on and under the surface of the thin plate are equal, the vibration equations of this electromagnetic-mechanical coupled thin plate can be written as follows (Xu, 1988; Bai, 1996b):

$$\begin{aligned}
&\frac{\partial N_1}{\partial x}+\frac{\partial N_{12}}{\partial y}+(P_1+\rho f_1)=\rho h\frac{\partial^2 u}{\partial t^2},\\
&\frac{\partial N_2}{\partial y}+\frac{\partial N_{12}}{\partial x}+(P_2+\rho f_2)=\rho h\frac{\partial^2 v}{\partial t^2},\\
&\frac{\partial Q_1}{\partial x}+\frac{\partial Q_2}{\partial y}+(P_3+\rho f_3)=\rho h\frac{\partial^2 w}{\partial t^2},\\
&\frac{\partial M_1}{\partial x}+\frac{\partial M_{12}}{\partial y}+N_1\theta_1+N_{12}\theta_2-Q_1+m_1=\frac{\rho h^3}{12}\frac{\partial\theta_1^2}{\partial t^2},\\
&\frac{\partial M_2}{\partial y}+\frac{\partial M_{12}}{\partial x}+N_2\theta_2+N_{12}\theta_1-Q_2+m_2=\frac{\rho h^3}{12}\frac{\partial\theta_2^2}{\partial t^2},
\end{aligned}\tag{1}$$

where N_1, N_2, N_{12} are the elements of the internal force vector in the neutral layer of the thin plate; M_1, M_2, M_{12} are the elements of the internal moment vector in the neutral layer of the thin plate; $w(x, y)$ is the displacement in z direction of the neutral plate; P_1, P_2, P_3 are the mechanical forces in z direction; h is the thickness of the thin plate; ρ is the specific mass; Q_1, and Q_2 are the internal forces of the flexible plate.

In Eq.(1), ρf_1, ρf_2, ρf_3 and m_1, m_2 are Lorenz forces and moments (Bai, 1996b), and they are written as follows:

$$\begin{aligned}
\rho f_1&=\sigma h B_z\left(e_y+\frac{\partial w}{\partial t}B_x-\frac{\partial u}{\partial t}B_z\right),\\
\rho f_2&=\sigma h B_z\left(-e_x+\frac{\partial w}{\partial t}B_y-\frac{\partial v}{\partial t}B_z\right),\\
\rho f_3&=\sigma h B_y\left(e_x-\frac{\partial w}{\partial t}B_y+\frac{\partial v}{\partial t}B_z\right)\\
&\quad-\sigma h B_x\left(e_y+\frac{\partial w}{\partial t}B_x-\frac{\partial u}{\partial t}B_z\right),\\
m_1&=\frac{\sigma h^3}{12}B_z^2\frac{\partial^2 w}{\partial t\partial x},\ m_2=\frac{\sigma h^3}{12}B_z^2\frac{\partial^2 w}{\partial t\partial y},
\end{aligned}\tag{2}$$

where e_x, e_y, e_z are the elements of electrical field

intensity; E is the modulus of elasticity; t is the time; σ is the electrical conductivity; B_z is the electromagnetic field intensity in z direction.

The stretch equations and geometry equations are (Xu, 1988)

$$\begin{aligned}
&N_1 = D_N(\varepsilon_1 + \nu\varepsilon_2),\ N_2 = D_N(\varepsilon_2 + \nu\varepsilon_1),\\
&N_{12} = D_N\Omega(1-\nu)/2,\ M_1 = D_M(\kappa_1 + \nu\kappa_2),\\
&M_2 = D_M(\kappa_2 + \nu\kappa_1),\ M_{12} = D_M(1-\nu)\tau; \qquad (3)\\
&\varepsilon_1 = \frac{\partial u}{\partial x} + \frac{1}{2}\left(\frac{\partial w}{\partial x}\right)^2,\ \varepsilon_2 = \frac{\partial v}{\partial y} + \frac{1}{2}\left(\frac{\partial w}{\partial y}\right)^2,\\
&\kappa_1 = -\frac{\partial^2 w}{\partial x^2},\ \kappa_2 = -\frac{\partial^2 w}{\partial y^2},\\
&\tau = -\frac{\partial^2 w}{\partial x\partial y},\ \Omega = \frac{\partial v}{\partial x} + \frac{\partial u}{\partial y} + \frac{\partial w}{\partial x}\frac{\partial w}{\partial y}, \qquad (4)
\end{aligned}$$

where D_N is the extensional rigidity of the plate, D_M is the flexural rigidity of the plate, ν is the Poisson's ratio.

By substituting Eqs.(2)~(4) into Eq.(1), ignoring inertial effects and considering its nonlinear geometry, the simplified vibration equations of the thin plate can be written as follows:

$$\begin{aligned}
&D_M\nabla^4 w + \frac{D_N}{2}\left[3\frac{\partial^2 w}{\partial x^2}\left(\frac{\partial w}{\partial x}\right)^2 + \frac{\partial^2 w}{\partial x^2}\left(\frac{\partial w}{\partial y}\right)^2\right.\\
&\left.+\left(\frac{\partial w}{\partial x}\right)^2\frac{\partial^2 w}{\partial y^2} + 3\frac{\partial^2 w}{\partial y^2}\left(\frac{\partial w}{\partial y}\right)^2 + 4\frac{\partial w}{\partial x}\frac{\partial w}{\partial y}\frac{\partial^2 w}{\partial x\partial y}\right] \qquad (5)\\
&-\frac{\sigma h^3}{12}B_z^2\frac{\partial(\nabla^2 w)}{\partial t} + \rho h\frac{\partial^2 w}{\partial t^2} - P_3 = 0,
\end{aligned}$$

where

$$\nabla^4 = \frac{\partial^4}{\partial x^4} + 2\frac{\partial^4}{\partial x^2\partial y^2} + \frac{\partial^4}{\partial y^4},\ \nabla^2 = \frac{\partial^2}{\partial x^2} + \frac{\partial^2}{\partial y^2},$$

$$D_N = \frac{Eh}{1-\nu^2},\ D_M = \frac{Eh^3}{12(1-\nu^2)}.$$

The schematic diagram for a 4-side clamped rectangular thin plate loaded in the transverse steady electromagnetic field $\overline{\boldsymbol{B}}(0, 0, B_z)$ and transverse uniformly distributed mechanical force $\overline{\boldsymbol{P}}(0, 0, P_3)$ is shown in Fig.1.

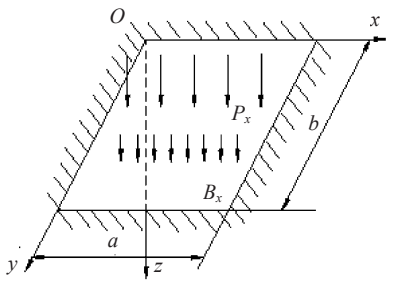

Fig.1 Model of thin rectangular plate

The boundary conditions are

$$\begin{aligned}
&w(0, y) = w(a, y) = 0,\\
&\left.\frac{\partial w}{\partial x}\right|_{(0,y)} = \left.\frac{\partial w}{\partial x}\right|_{(a,y)} = 0;\\
&w(x, 0) = w(x, b) = 0,\\
&\left.\frac{\partial w}{\partial y}\right|_{(x,0)} = \left.\frac{\partial w}{\partial y}\right|_{(x,b)} = 0. \qquad (6)
\end{aligned}$$

Assuming that the solution of Eq.(5) is

$$W(x, y, t) = \phi(t)w(x, y), \qquad (7)$$

where $w(x,y)$ is the first order dominant mode of vibration given by

$$w(x, y) = \left[1 - \cos\left(\frac{2\pi}{a}x\right)\right]\left[1 - \cos\left(\frac{2\pi}{b}y\right)\right]. \qquad (8)$$

The mechanical loads are assumed two kinds:

$$\text{(i)}\ P_3 = p\cos(\omega t), \qquad (9a)$$

$$\text{(ii)}\ P_3 = p\left[1 - \cos\left(\frac{2\pi}{a}x\right)\right]\left[1 - \cos\left(\frac{2\pi}{b}y\right)\right]\cos(\omega t), \qquad (9b)$$

where p is the amplitude of the mechanical load.

Substituting Eqs.(8) and Eq.(9a) or Eq.(9b) into Eq.(5), we obtain Eq.(10a) and Eq.(10b); Integrating Eq.(10) by the Galerkin's method, we have Eq.(11a) and Eq.(11b) as follows:

$$D_M\left\{-\left(\frac{2\pi}{a}\right)^4\cos\left(\frac{2\pi}{a}x\right)\left[1-\cos\left(\frac{2\pi}{b}y\right)\right]+2\left(\frac{2\pi}{a}\right)^2\left(\frac{2\pi}{b}\right)^2\cos\left(\frac{2\pi}{a}x\right)\cos\left(\frac{2\pi}{a}y\right)\right.$$
$$\left.-\left(\frac{2\pi}{b}\right)^4\cos\left(\frac{2\pi}{b}x\right)\left[1-\cos\left(\frac{2\pi}{a}y\right)\right]\right\}\phi(t)+\frac{D_N}{2}\left\{3\left(\frac{2\pi}{a}\right)^4\sin^2\left(\frac{2\pi}{a}x\right)\cos\left(\frac{2\pi}{a}x\right)\left[1-\cos\left(\frac{2\pi}{b}y\right)\right]^3\right.$$
$$+\left(\frac{2\pi}{a}\right)^2\left(\frac{2\pi}{b}\right)^2\cos\left(\frac{2\pi}{a}x\right)\left[1-\cos\left(\frac{2\pi}{a}x\right)\right]^2\sin^2\left(\frac{2\pi}{b}y\right)\left[1-\cos\left(\frac{2\pi}{b}y\right)\right]+\left(\frac{2\pi}{a}\right)^2\left(\frac{2\pi}{b}\right)^2\sin^2\left(\frac{2\pi}{a}x\right)$$
$$\cdot\left[1-\cos\left(\frac{2\pi}{a}x\right)\right]\cos\left(\frac{2\pi}{b}y\right)\left[1-\cos\left(\frac{2\pi}{b}y\right)\right]^2+3\left(\frac{2\pi}{b}\right)^4\left[1-\cos\left(\frac{2\pi}{a}x\right)\right]^3\sin^2\left(\frac{2\pi}{b}y\right)\cos\left(\frac{2\pi}{b}y\right)$$
$$+4\left(\frac{2\pi}{a}\right)^2\left(\frac{2\pi}{b}\right)^2\sin^2\left(\frac{2\pi}{a}x\right)\left[1-\cos\left(\frac{2\pi}{a}x\right)\right]\sin^2\left(\frac{2\pi}{b}y\right)$$
$$\left.\cdot\left[1-\cos\left(\frac{2\pi}{b}y\right)\right]\right\}\phi^3(t)-\frac{\sigma h^3}{12}B_z^2\left\{\left(\frac{2\pi}{a}\right)^2\cos\left(\frac{2\pi}{a}x\right)\left[1-\cos\left(\frac{2\pi}{b}y\right)\right]+\left(\frac{2\pi}{b}\right)^2\left[1-\cos\left(\frac{2\pi}{a}x\right)\right]\right.$$
$$\left.\cdot\cos\left(\frac{2\pi}{b}y\right)\right\}\phi(t)+\rho h\ddot{\phi}(t)\left[1-\cos\left(\frac{2\pi}{a}x\right)\right]\left[1-\cos\left(\frac{2\pi}{b}y\right)\right]-p\cos(\omega t)=0, \tag{10a}$$

$$D_M\left\{-\left(\frac{2\pi}{a}\right)^4\cos\left(\frac{2\pi}{a}x\right)\left[1-\cos\left(\frac{2\pi}{b}y\right)\right]+2\left(\frac{2\pi}{a}\right)^2\left(\frac{2\pi}{b}\right)^2\cos\left(\frac{2\pi}{a}x\right)\cos\left(\frac{2\pi}{b}y\right)\right.$$
$$\left.-\left(\frac{2\pi}{b}\right)^4\cos\left(\frac{2\pi}{b}x\right)\left[1-\cos\left(\frac{2\pi}{a}y\right)\right]\right\}\phi(t)+\frac{D_N}{2}\left\{3\left(\frac{2\pi}{a}\right)^4\sin^2\left(\frac{2\pi}{a}x\right)\cos\left(\frac{2\pi}{a}x\right)\left[1-\cos\left(\frac{2\pi}{b}y\right)\right]^3\right.$$
$$+\left(\frac{2\pi}{a}\right)^2\left(\frac{2\pi}{b}\right)^2\cos\left(\frac{2\pi}{a}x\right)\left[1-\cos\left(\frac{2\pi}{a}x\right)\right]^2\sin^2\left(\frac{2\pi}{b}y\right)\left[1-\cos\left(\frac{2\pi}{b}y\right)\right]+\left(\frac{2\pi}{a}\right)^2\left(\frac{2\pi}{b}\right)^2\sin^2\left(\frac{2\pi}{a}x\right)$$
$$\cdot\left[1-\cos\left(\frac{2\pi}{a}x\right)\right]\cos\left(\frac{2\pi}{b}y\right)\left[1-\cos\left(\frac{2\pi}{b}y\right)\right]^2+3\left(\frac{2\pi}{b}\right)^4\left[1-\cos\left(\frac{2\pi}{a}x\right)\right]^3\sin^2\left(\frac{2\pi}{b}y\right)\cos\left(\frac{2\pi}{b}y\right)$$
$$\left.+4\left(\frac{2\pi}{a}\right)^2\left(\frac{2\pi}{b}\right)^2\sin^2\left(\frac{2\pi}{a}x\right)\left[1-\cos\left(\frac{2\pi}{a}x\right)\right]\sin^2\left(\frac{2\pi}{b}y\right)\left[1-\cos\left(\frac{2\pi}{b}y\right)\right]\right\}\phi^3(t)$$
$$-\frac{\sigma h^3}{12}B_z^2\left\{\left(\frac{2\pi}{a}\right)^2\cos\left(\frac{2\pi}{a}x\right)\left[1-\cos\left(\frac{2\pi}{b}y\right)\right]+\left(\frac{2\pi}{b}\right)^2\left[1-\cos\left(\frac{2\pi}{a}x\right)\right]\cos\left(\frac{2\pi}{b}y\right)\right\}\phi(t)$$
$$+\rho h\ddot{\phi}(t)\left[1-\cos\left(\frac{2\pi}{a}x\right)\right]\left[1-\cos\left(\frac{2\pi}{b}y\right)\right]-p\left[1-\cos\left(\frac{2\pi}{a}x\right)\right]\left[1-\cos\left(\frac{2\pi}{b}y\right)\right]\cos(\omega t)=0; \tag{10b}$$

$$D_M\left\{2\left(\frac{2\pi}{a}\right)^4+2\left(\frac{2\pi}{b}\right)^4+\left[\left(\frac{2\pi}{a}\right)^2+\left(\frac{2\pi}{b}\right)^2\right]^2\right\}\phi(t)+105\left(\frac{2\pi}{b}\right)^4\phi^3(t)+\frac{\sigma h^3}{4}B_z^2\left[\left(\frac{2\pi}{a}\right)^2+\left(\frac{2\pi}{b}\right)^2\right]\dot{\phi}(t)$$
$$+9\rho h\ddot{\phi}(t)-4p\cos(\omega t)=0, \tag{11a}$$

$$D_M\left\{2\left(\frac{2\pi}{a}\right)^4+2\left(\frac{2\pi}{b}\right)^4+\left[\left(\frac{2\pi}{a}\right)^2+\left(\frac{2\pi}{b}\right)^2\right]^2\right\}\phi(t)+105\left(\frac{2\pi}{b}\right)^4\phi^3(t)+\frac{\sigma h^3}{4}B_z^2\left[\left(\frac{2\pi}{a}\right)^2+\left(\frac{2\pi}{b}\right)^2\right]\dot{\phi}(t)$$
$$+9\rho h\ddot{\phi}(t)-9p\cos(\omega t)=0. \tag{11b}$$

Suppose

$$a_1=\left(\frac{2\pi}{a}\right)^2+\left(\frac{2\pi}{b}\right)^2,$$

$$a_2=2\left(\frac{2\pi}{a}\right)^4+2\left(\frac{2\pi}{b}\right)^4+\left[\left(\frac{2\pi}{a}\right)^2+\left(\frac{2\pi}{b}\right)^2\right]^2,$$

$$a_3=105\left(\frac{2\pi}{a}\right)^4+50\left(\frac{2\pi}{a}\right)^2\left(\frac{2\pi}{b}\right)^2+105\left(\frac{2\pi}{b}\right)^4,$$

$$\mu=\frac{\sigma h^2 Bz^2 a_1}{36\rho},\quad \alpha=\frac{D_M a_2}{9\rho h},$$

$$\beta=\frac{D_N a_3}{288\rho h},\ F=\frac{4p}{9\rho h}\text{ or }F=\frac{p}{\rho h}.$$

Then Eq.(11) can be rewritten as

$$\ddot{\phi}+\mu\dot{\phi}+\alpha\phi+\beta\phi^3-F\cos(\omega t)=0. \tag{12}$$

Assuming

$$x=\sqrt{\frac{\beta}{\alpha}}\phi,\quad \tau=\sqrt{\alpha}t,$$

$$\omega_0=\frac{\omega}{\sqrt{\alpha}},\quad \gamma=\frac{\mu}{\alpha},\quad f=\frac{\sqrt{\beta}}{\sqrt{\alpha}}F,$$

replacing τ with t, and using the non-dimensional method, Eq.(12) can be finally rewritten as

$$\ddot{x}+\gamma\dot{x}+x+x^3=f\cos(\omega_0 t). \tag{13}$$

MELNIKOV FUNCTION

Suppose $\dot{X}=Y$, $f=\varepsilon f_1$ and $\gamma=\varepsilon\gamma_1$, then the equivalent form of Eq.(13) can be written as

$$\begin{cases}\dot{X}=Y,\\ \dot{Y}=-X-X^3+\varepsilon(-\delta_1 Y+f_1\cos(\omega_0 t)).\end{cases} \tag{14}$$

When $\varepsilon=0$, i.e., $\delta=0$, $\gamma=0$, Eq.(14) is an unperturbed Hamiltonian system as

$$\begin{cases}\dot{X}=Y,\\ \dot{Y}=-X-X^3;\end{cases} \tag{15}$$

$$\begin{cases}\dot{X}=Y=0,\\ \dot{Y}=-X-X^3=0.\end{cases} \tag{16}$$

From Eq.(16) we get the solutions for three fixed points (1,0), (−1,0), and (0,0). Then we can obtain two hetero-clinic orbital parameter equations

$$\begin{cases}X_i(t)=\pm\tanh\left(\frac{1}{\sqrt{2}}t\right),\\ Y_i(t)=\pm\frac{1}{\sqrt{2}}\operatorname{sech}^2\left(\frac{1}{\sqrt{2}}t\right),\end{cases}\quad i=1,2. \tag{17}$$

According to the Melnikov theory, if $M_i(t_0)=0$, we have

$$\frac{\gamma_1}{\delta_1}=\frac{2}{3\pi\omega_0\operatorname{csch}\left(\frac{\pi\omega_0}{\sqrt{2}}\right)\cos(\omega_0 t_0)}. \tag{18}$$

Since $M_i(t_0)\neq 0$, $\cos(\omega_0 t_0)\neq\pm1$, i.e., $|\cos(\omega_0 t_0)|<1$, chaos motion of Eq.(1) under Smale horseshoe mapping may take place when

$$\frac{\gamma_1}{\delta_1}>\frac{2}{3\pi\omega_0\operatorname{csch}\left(\frac{\pi\omega_0}{\sqrt{2}}\right)}.$$

NUMERICAL RESULTS AND ANALYSIS

We take a thin aluminum plate as an example with the following parameters: $h=0.5\times10^{-3}$ m, $\rho=2700$ kg/m^3, $E=70$ GPa, $\nu=0.33$, $\sigma=3.6\times10^7$ $(\Omega\cdot\text{m})^{-1}$, $a=\pi/8$ m, $b=\pi/4$ m, $\omega_0=1$.

Then the non-dimensional parameters are calculated for the above values. The second order ordinary differential equation (ODE) Eq.(13) is transformed to the first order ODE, which are then solved by the fourth-order Runge-Kutta method. In the following numerical calculations, the sampling period is 300 rad and the integral tolerance error is 10^{-6}. In the simulation, we begin to interpret the results of integral time

response after repeating 800 times, which assures that the dynamic response of the system has achieved a steady state. These results include displacement, velocity, mechanical load, time, and so on, which will be used to plot the bifurcation diagram, phase diagram, wave diagram of displacement, Poincare section diagram and the Lyapunov exponent diagram.

1. $P_3=p\cos(\omega t)$

When ω_0=1 and B_z=1 T, we can obtain the global bifurcation diagram and the homologous Lyapunov exponent diagram of the thin plate system by modulating the value of p from 250 to 270 N/m^2, as shown in Figs.2 and 3. From these figures, it can be found that the system changes alternately between a state of periodic motion and chaos when the value of p is escalating. Figs.4~6 show the Poincare section diagram, the phase diagram and the wave diagram of displacement of the system with different values of p. For example, the system is in a chaotic motion state when p=252 N/m^2, but it is in a periodic state when p=256 N/m^2, and it is in a chaotic motion state again when the value of p increases to 266 N/m^2. This is a representative characteristic of the chaotic motion for the nonlinear system.

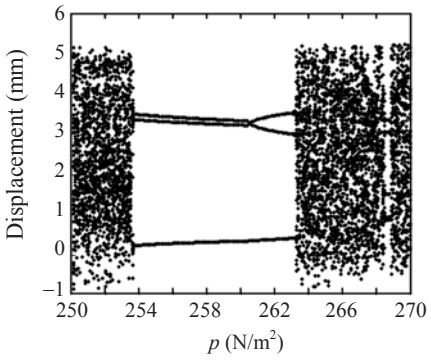

Fig.2 Bifurcation diagram (ω_0=1, B_z=1 T)

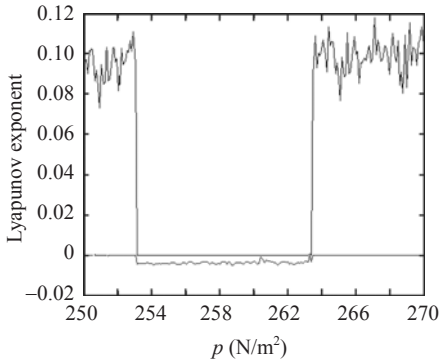

Fig.3 Lyapunov exponent diagram (ω_0=1, B_z=1 T)

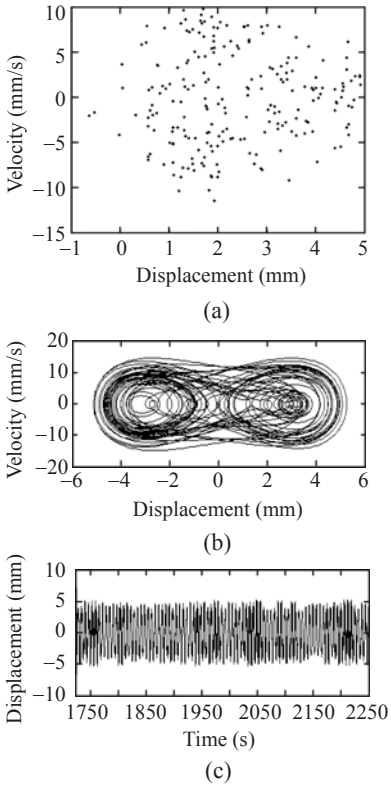

Fig.4 Poincare map (a), phase diagram (b) and wave diagram (c) of displacement (p=252 N/m^2)

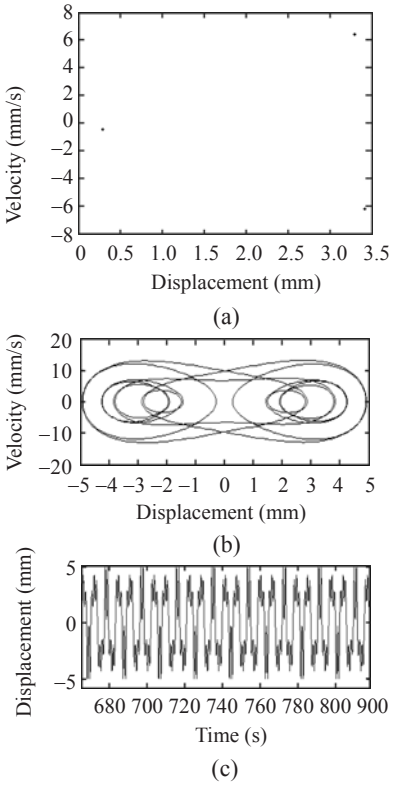

Fig.5 Poincare map (a), phase diagram (b) and wave diagram (c) of displacement (p=256 N/m^2)

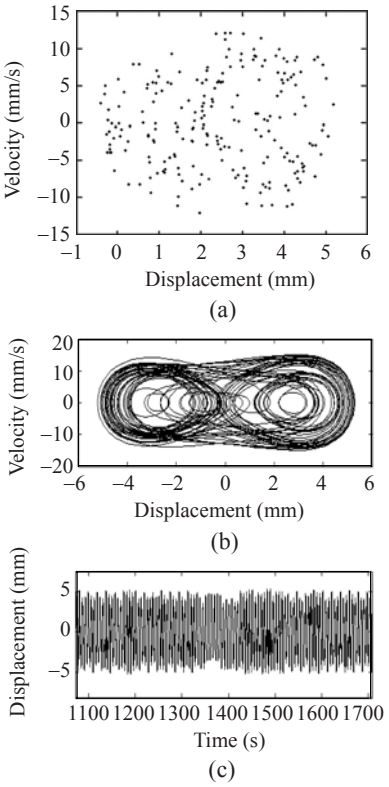

Fig.6 Poincare map (a), phase diagram (b) and wave diagram (c) of displacement (p=266 N/m^2)

We can obtain the global bifurcation diagram and homologous Lyapunov exponent diagram of the thin plate system by modulating the value of B_z from 0 to 2 T, as shown in Figs.7 and 8, taking ω_0=1 and p=258 N/m^2. The figures show that the electromagnetic intensity B_z has an obvious influence on the motion state of the system. Reducing B_z (less than 1 T), the system is in a chaotic motion state. Figs.9 and 10 denote the Poincare section diagram, the phase diagram and the wave diagram of displacement of the system with different values of B_z. So the value of B_z must be not too small if we want to eliminate the influence of B_z on chaotic motion for this system.

When p=258 N/m^2 and B_z=1.0 T, we can obtain the global bifurcation diagram of the thin plate system by modulating the value of ω_0 from 0.7 to 1.5 (Fig.11). It shows that the value of ω_0 has a global influence on the motion state of the system. The system changes alternately between periodic motion and chaotic motion as the value of ω_0 increases. Figs.12~14 show the Poincare section diagram, phase diagram and wave diagram of displacement for this system with different values of ω_0.

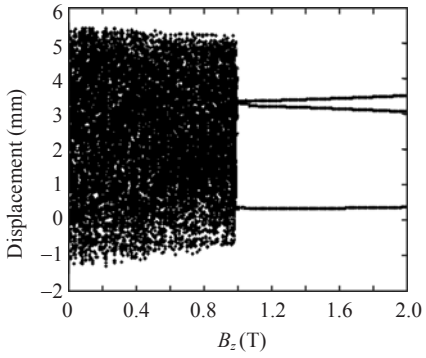

Fig.7 Bifurcation diagram (ω_0=1, p=258 N/m^2)

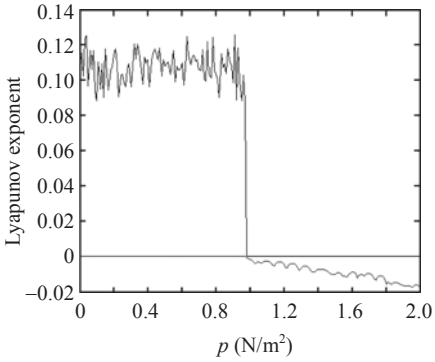

Fig.8 Lyapunov exponent diagram (ω_0=1, p=258 N/m^2)

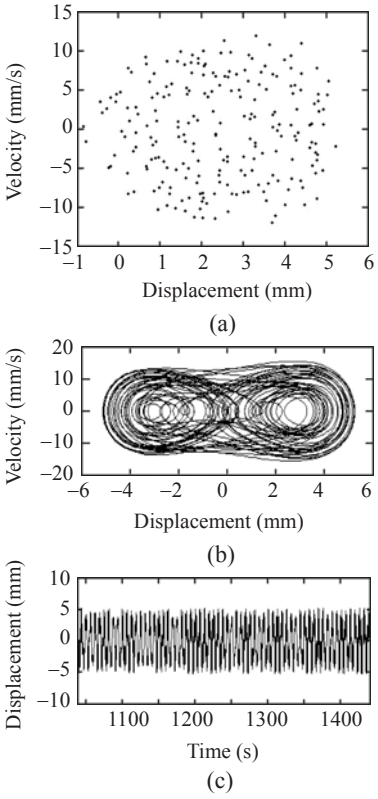

Fig.9 Poincare map (a), phase diagram (b) and wave diagram (c) of displacement (B_z=0.5 T)

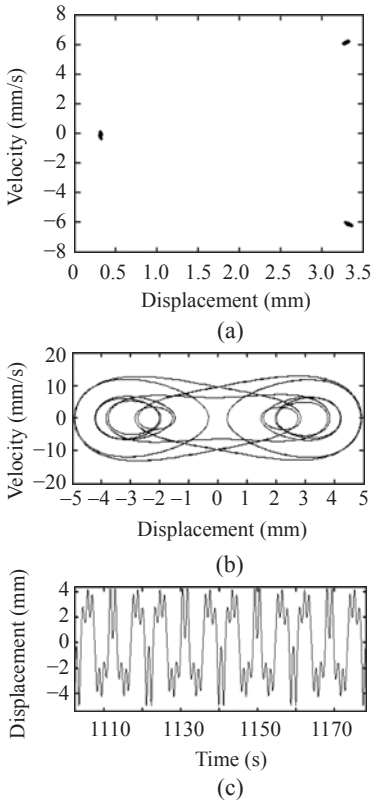

Fig.10 Poincare map (a), phase diagram (b) and wave diagram (c) of displacement (B_z=1.2 T)

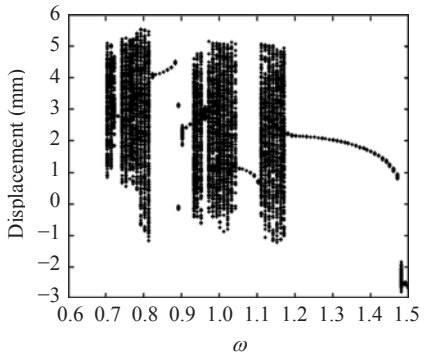

Fig.11 Bifurcation diagram (p=258 N/m^2, B_z=1.2 T)

$$2.\ P_3 = p\left[1-\cos\left(\frac{2\pi}{a}x\right)\right]\left[1-\cos\left(\frac{2\pi}{b}y\right)\right]\cos(\omega t)$$

The only difference between Eqs.(11a) and (11b) is the coefficient of p. The global bifurcation and the homologous Lyapunov exponent of the thin plate system are investigated. Firstly we get Figs.15 and 16 by modulating the value of p from 175 to 210 N/m^2. Secondly we draw Figs.17 and 18 by modulating the value of ω_0 from 0.4 to 1.6. Finally Figs.19 and 20 are obtained by modulating the value of B_z from

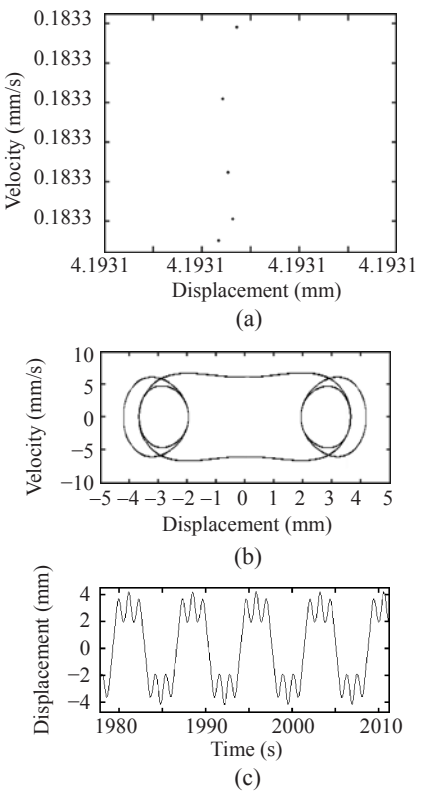

Fig.12 Poincare map (a), phase diagram (b) and wave diagram (c) of displacement (ω_0=0.85)

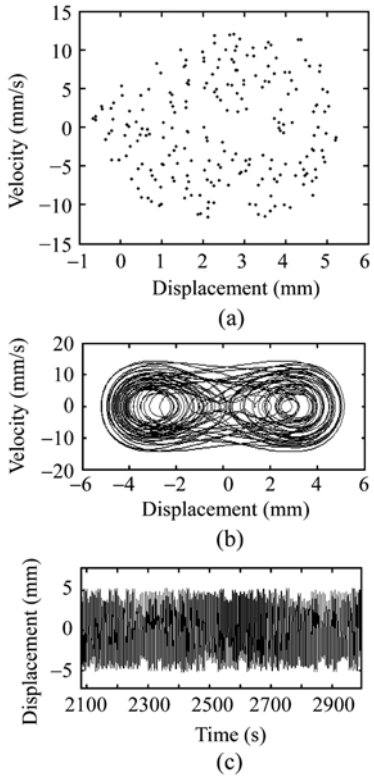

Fig.13 Poincare map (a), phase diagram (b) and wave diagram (c) of displacement (ω_0=1.0)

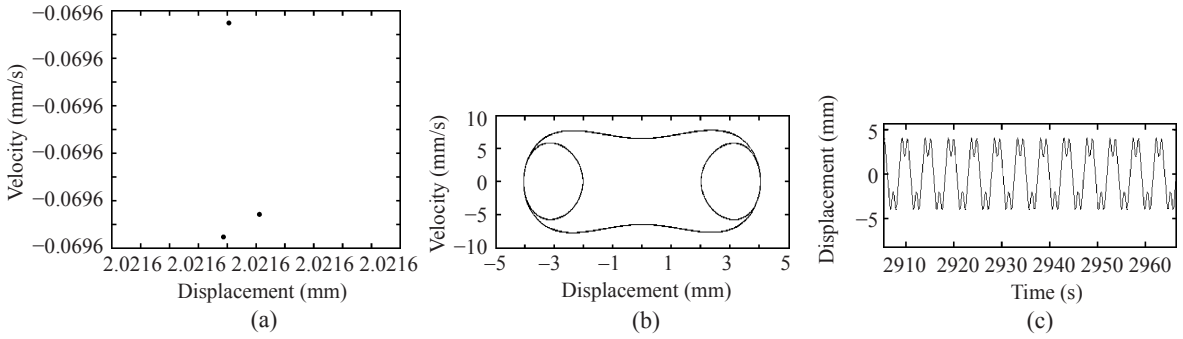

Fig.14 Poincare map (a), phase diagram (b) and wave diagram (c) of displacement (ω_0=1.3)

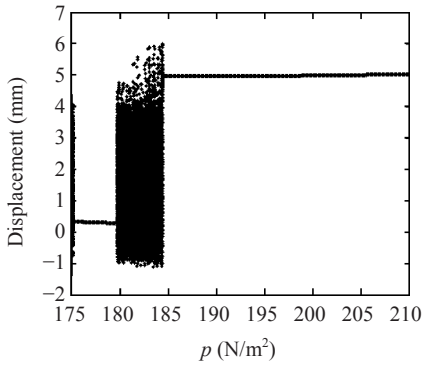

Fig.15 Bifurcation diagram (ω_0=1.0, B_z=1.0 T)

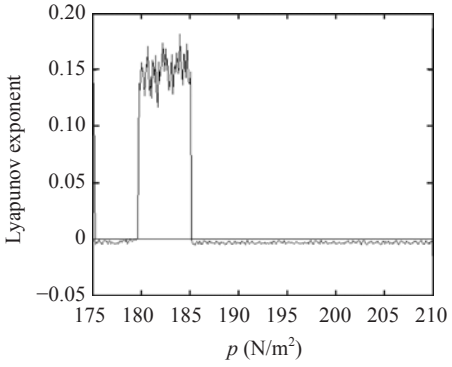

Fig.16 Lyapunov exponent diagram (ω_0=1.0, B_z=1.0 T)

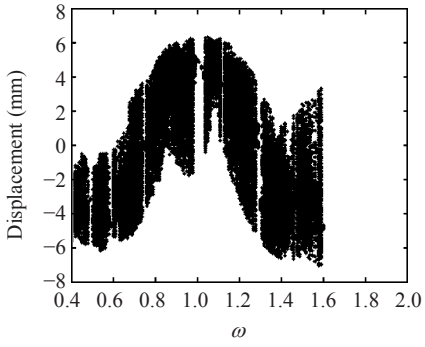

Fig.17 Bifurcation diagram (p=100 N/m^2, B_z=1.0 T)

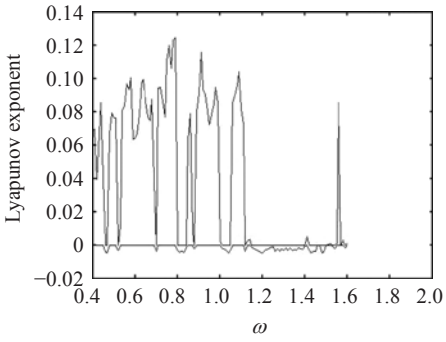

Fig.18 Lyapunov exponent diagram (p=100 N/m^2, B_z=1.0 T)

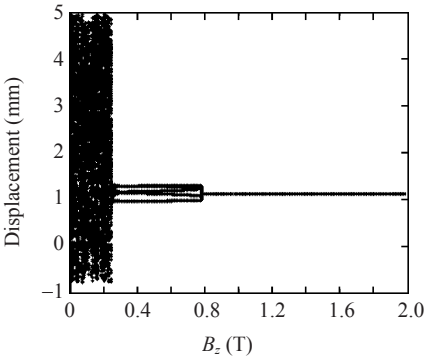

Fig.19 Bifurcation diagram (ω_0=1.0, p=100 N/m^2)

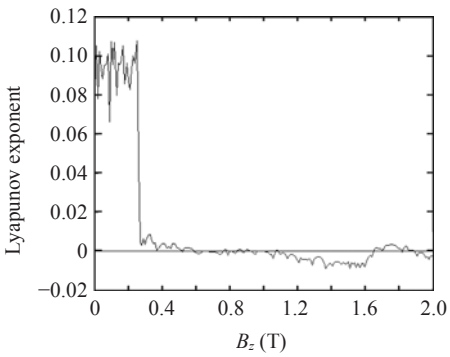

Fig.20 Lyapunov exponent diagram (ω_0=1.0, p=100 N/m^2)

0 to 2 T. It can be found that the system always changes alternately between periodic motion and chaotic motion in the three cases.

CONCLUSION

The vibration equations for the rectangular thin plate in electromagnetic and mechanical fields are obviously non-linear. When the amplitude p and frequency ω_0 of mechanical load are changed, the system's motion characteristics are comparatively complicated with two different kinds of incentive loads p_3, and the system would change alternately between periodic motion and chaotic motion. The electromagnetic intensity B_z has an obvious influence on the motion state of the system. Since the system is in chaotic motion as B_z is reduced (less than 1 T), the value of B_z must not be too small if it needs to eliminate the influence of B_z on chaotic motion in this system. Thus, we can control the oscillation characteristics of the thin plate system and make the system to turn chaotic motion or to avoid chaos by modulating the mechanical loading, exciting the force frequency and electromagnetic parameters. It provides some values for the engineering design and safety.

References

Awrejcewicz, J., Krysko, V.A., Narkaitis, G.G., 2003. Bifurcations of a thin plate-strip excited transversally and axially. *Nonlinear Dynamics*, **32**(2):187-209. [doi:10.1023/A:1024458814785]

Awrejcewicz, J., Krysko, V.A., Krysko, A.V., 2004. Complex parametric vibrations of flexible rectangular plates. *Mechanicals*, **39**(3):221-244.

Awrejcewicz, J., Krysko, V.A., Narkaitis, G.G., 2006. Nonlinear vibration and characteristics of flexible plate-strips with non-symmetric boundary conditions. *Communications in Nonlinear Science and Numerical Simulation*, **11**(1):95-124. [doi:10.1016/j.cnscn.2003.11.002]

Bai, X.Z., 1996a. Magnetoelasticity, thermal-magnetoelasticity and their applications. *Advances in Mechanicals*, **26**(3):389-406 (in Chinese).

Bai, X.Z., 1996b. Basic Elastic-magnetic Theory of Plate and Shell. Machinery Industry Publishing House, Beijing (in Chinese).

Chang, W.P., Wang, S.M., 1986. Thermo-mechanicalally coupled nonlinear vibration of plates. *International Journal of Non-Linear Mechanics*, **21**(5):375-389. [doi:10.1016/0020-7462(86)90021-1]

Chen, Y.S., 1993. Bifurcation and Chaos Theory of Nonlinear Oscillation System. Higher Education Publishing House, Beijing (in Chinese).

Huang, R.S., 2000. Chaos and Application. Wuhan University Publishing Company, Wuhan (in Chinese).

Nowacki, W., 1975. Dynamic Problems of Thermo-elasticity. Sijthoff and Noordhoff International Publishers, Leyden, p.123-262.

Pan, E., 2001. Exact solution for simply supported and multilayered magneto-electro-elastic plate. *ASME Journal of Applied Mechanicals*, **68**:608-618.

Pan, E., Heyliger, P.R., 2002. Free vibrations of simply supported and multilayered magneto-electro-elastic plates. *Journal of Sound and Vibration*, **252**(3):429-442. [doi:10.1006/jsvi.2001.3693]

Pan, E., Han, F., 2005. Exact solution for functionally graded and layered magneto-electro-elastic plates. *International Journal of Engineering Science*, **43**(3-4):321-339. [doi:10.1016/j.ijengsci.2004.09.006]

Trajkorski, D., Cukic, R., 1999. A coupled problem of thermo-elastic vibrations of a circular plate with exact boundary conditions. *Mechanics Research Communications*, **26**(2):217-224. [doi:10.1016/S0093-6413(99)00016-6]

Wang, J.G., Chen, L.F., Fang, S.S., 2003. State vector approach to analysis of multilayered magneto-electro-elastic plates. *International Journal of Solids and Structures*, **40**(7):1669-1680. [doi:10.1016/S0020-7683(03)00027-1]

Xu, Z.L., 1988. Elasticity. Higher Education Publishing House, Beijing (in Chinese).

Zhang, W., Liu, Z.M, Yu, P., 2001. Global dynamics of a parametrically and externally excited thin plate. *Nonlinear Dynamics*, **24**(3):245-268. [doi:10.1023/A:1008381718839]